Rapid and Simple Kinetics Screening Assay for Electrophilic Dermal Sensitizers Using Nitrobenzenethiol

Itai Chipinda,*[,†] Risikat O. Ajibola,[‡] Moshood K. Morakinyo,[‡] Tinashe B. Ruwona,[†,‡] Reuben H. Simoyi,[‡] and Paul D. Siegel[†]

Health Effects Laboratory Division, National Institute for Occupational Safety and Health, 1095 Willowdale Road, Morgantown, West Virginia 26505-2888, and Department of Chemistry, Portland State University, Portland, Oregon 97207-0751

Received January 7, 2010

The need for alternatives to animal-based skin sensitization testing has spurred research on the use of in vitro, in silico, and in chemico methods. Glutathione and other select peptides have been used to determine the reactivity of electrophilic allergens to nucleophiles, but these methods are inadequate to accurately measure rapid kinetics observed with many chemical sensitizers. A kinetic spectrophotometric assay involving the reactivity of electrophilic sensitizers to nitrobenzenethiol was evaluated. Stopped-flow techniques and conventional UV spectrophotometric measurements enabled the determination of reaction rates with half-lives ranging from 0.4 ms (benzoquinone) to 46.2 s (ethyl acrylate). Rate constants were measured for seven extreme, five strong, seven moderate, and four weak/nonsensitizers. Seventeen out of the 23 tested chemicals were pseudo-first order, and three were second order. In three out of the 23 chemicals, deviations from first and second order were apparent where the chemicals exhibited complex kinetics whose rates are mixed order. The reaction rates of the electrophiles correlated positively with their EC3 values within the same mechanistic domain. Nonsensitizers such as benzaldehyde, sodium lauryl sulfate, and benzocaine did not react with nitrobenzenethiol. Cyclic anhydrides, select diones, and aromatic aldehydes proved to be false negatives in this assay. The findings from this simple and rapid absorbance model show that for the same mechanistic domain, skin sensitization is driven mainly by electrophilic reactivity. This simple, rapid, and inexpensive absorbance-based method has great potential for use as a preliminary screening tool for skin allergens.

Introduction

Skin sensitization to chemicals present in consumer products and the workplace continues to be a major concern. Although current regulatory guidelines call for the identification of skin sensitizers to be performed through the murine local lymph node assay (LLNA) (*1*), the Buehler test (*2*), and the guinea pig maximization test (GPMT) (*3*), which are all animal-based, there is impetus within industry and European Union regulatory authorities to develop alternative nonanimal-based methods wherever possible. Alternative methods utilizing the chemical reactivity of test chemicals as end point toxicology assays have been proposed using current mechanistic understanding of the chemical and biological basis of skin sensitization (*4*). From a skin sensitization perspective, understanding and predicting early allergenic events, such as protein haptenation, are critical as discussed by Schultz et al. (*5*). A major and common factor in chemical-induced skin sensitization is the ability of a chemical, either as such or after ex/in cutaneo activation, to covalently react with a carrier protein or peptide (*6*), resulting in an immunogenic complex. This reactivity of chemicals to cutaneous proteins is the basis for most, if not all, current nonanimal-based methods. While the complete proteinaceous constituents of the skin are yet to be delineated (*7*), the development of in chemico methods, premised on protein haptenation, as end point skin sensitization predictive assays has shown promise. The interaction of skin sensitizers with proteins, peptides, and model nucleophiles representing cutaneously available proteins has been reported to be predominantly covalent bonding between electrophiles (E^+) and nucleophiles. For example, irreversible binding of dinitrochlorobenzene (DNCB), a known electrophilic skin sensitizer, to human serum albumin, cytokeratin 14, and cofilin (*8*) was demonstrated to be the rate-determining step in skin sensitization for DNCB. The reactivity of electrophilic chemicals to glutathione (GSH) was exploited by Schultz et al. (*9*) with the determination of the RC_{50} value being the marker of the potency of a chemical. RC_{50} was defined as the concentration of electrophile required to deplete 50% of the thiol group on GSH in 2 h. The peptide depletion assay developed by Gerberick et al. (*10, 11*) reported the identification of chemicals as skin sensitizers based on their ability to deplete GSH and nucleophilic heptapeptides. This method (*10*) measured the depletion of the peptides after treatment with excess electrophile for 24 h and adopted the percent depletion (dp) as the reactivity index of a given chemical. As a modification to the peptide reactivity assay (*10*), quantitative LC-MS was exploited by Natsch et al. (*12*) to characterize adduct formation as well as oxidation of the heptapeptide Cor1-C420 by skin sensitizers. Further modifications (*6, 13*) on the original HPLC assay (*10*) and the work of Natsch et al. (*12*) were performed by generating data on dp values based on varying initial concentrations (E_0) of the suspect compounds. Both the derivation of the RC_{50} (2 h assay) (*9*) and the dp (24 h assay) (*10*) values as reactivity indices, while promising as skin-sensitizing predictive methods, do not adequately capture the nature of the

* To whom correspondence should be addressed. E-mail: IChipinda@cdc.gov.
† National Institute for Occupational Safety and Health.
‡ Portland State University.

10.1021/tx100003w
Published on Web 04/19/2010

chemical kinetics involved in these electrophile−nucleophile interactions. RC_{50} and dp values measured at fixed time points using initial test compound concentrations result in imprecise rate constants as different chemicals with different reactivities are bound to give complete depletion of the peptides after several hours. The initial reaction and chemical kinetics involved have a bearing on whether the reaction with the peptide is going to be linear or not throughout its duration, an aspect that is overlooked by both the GSH and peptide reactivity assays. A recent review proffers a detailed argument on the shortcomings of these assays (*6*).

The high-throughput kinetic profiling (HTKP) method reported by Roberts and Natsch (*14*) improved the earlier assays and addressed some of the pitfalls with respect to reaction times and deviations by some sensitizers from ideal behavior. The HTKP method compiled data on the depletion of the thiol group of the heptapeptide Ac-RFAACAA. To address the range of reaction times, measurements of peptide depletion were done at several different time points for varying initial concentrations (E_0) of the sensitizers. Models were proposed to compensate for the "drowning out effect" (*14*) and loss of test chemicals due to evaporation. Despite these improvements, the HTKP model still failed to accurately measure the kinetics of very reactive compounds like 2-methyl-4-isothiazolinone and benzoquinone (*14*).

In this paper, we present a novel kinetic spectrophotometric chemoassay for the assessment of skin sensitizers by reactivity toward 4-nitrobenzenethiol (NBT). Stopped-flow techniques and conventional UV absorbance measurements were used to determine rate constants of reactions ranging from seconds to hours to reach completion. Data generated from this simple and rapid absorbance model are correlated with LLNA-derived skin sensitization potency within the same mechanistic domain.

Materials and Methods

Chemicals. Phosphate buffer, acetic acid, sodium acetate, acetonitrile (ACN), acetone, NBT, and all test chemicals were purchased from Sigma Chemical Co. (St. Louis, MO).

UV/Vis Spectroscopy. Absorbance measurements were carried out on a Beckman DU 800 Spectrophotometer using quartz cells with calibrated 1 cm path lengths. Experiments were carried out at 25 °C with the temperature controlled by a VWR Scientific circulating water bath.

Stopped-Flow Studies. Rapid reactions were performed on a Hitech Scientific SF-61DX2 double-mixing stopped-flow spectrophotometer with an F/4 Czerny-Turner MG-60 monochromator and a spectra scan control unit. The signal from the spectrophotometer was amplified and digitized via an Omega Engineering DAS-50/1 16-bit A/D board interfaced to a computer for storage and data analysis. The reaction progress was followed by monitoring the loss of free thiol on NBT at 412 nm, where it has its highest molar absorptivity coefficient (ε).

Test chemicals were dissolved in ACN (and acetone for TDI and DPCP) at concentrations ranging from 0.01 to 10 mM. These solutions (5 μL) were combined with 5 μL of 0.1 mM NBT in 100 mM phosphate buffer (pH 7.4) in a sealed reaction cell with rapid mixing. Absorbance readings were collected after a dead time of 1 ms. Control experiments contained ACN and phosphate buffer only to determine background absorbance. Five replicates were performed for each chemical at each concentration. The temperature was maintained at 25 °C in the observation cell with a VWR Scientific circulating water bath. Twenty known dermal sensitizers and three nonsensitizers (Table 1) were used to evaluate the potential of this kinetic assay for the identification of contact allergens.

Results

Depletion of the highly absorbing chromophore, NBT, was measured after rapid mixing with test electrophiles. For every mole of NBT reacted, 1 mol of the electrophile was consumed assuming that the reactions were all going in the forward direction and to completion. TDI was an exception with two electrophilic centers that are amenable to thiol attack. The change in absorbance of the NBT with time was hence used to calculate the amount of free thiol remaining at time t, $[NBT]_t$, by using the following equation

$$[NBT]_t = \frac{A_{NBT_t}}{\varepsilon} \tag{1}$$

where A_{NBT_t} is the absorbance of the chromophore NBT at time t and ε ($11068 \pm 126\ M^{-1}\ cm^{-1}$) is its absorptivity coefficient where the path length is 1 cm.

Chemicals were classified into three mechanistic domains that are (i) Michael acceptors, (ii) S_N1/S_N2 reactants, and (iii) acylating agents. Figure 1i−iii shows the depletion of NBT during reaction with BQ, NBB, and TDI representing the Michael acceptor, S_N1/S_N2 reactants, and acylating agents, respectively. Where the electrophile was in excess over NBT, the time taken for the E^+−NBT reaction to reach completion ranged from <1 s (BQ) to >1 h (EA).

Kinetic studies were based on the working hypothesis that nucleophilic attack (by the NBT thiol group) on electron-deficient centers on the test chemical, leading to adduct formation, were the major reaction pathways. The order (with respect to E^+) and apparent rate constants ($k_0 = -k_a[NBT]_0$) were determined as the slope of the plot of several initial rates (R) against several $[E^+]_0$ for a fixed concentration of NBT.

$$R = \frac{d[NBT]}{dt} = -k_a[NBT]_0[E^+]_0 \tag{2}$$

As an illustrative example of the Michael acceptor domain, the initial rate plot for BQ is shown in Figure 2i. A good linear fit was obtained for several $[E^+]_0$ values and shows that the reaction is first order with respect to BQ. Using the apparent rate constants (k_0), the calculated rate constants (k) for BQ and other chemicals in the same domain are listed in Table 2a for a fixed [NBT]. The order of the reaction with respect to the electrophiles is also listed in Table 2a. Nitrobenzyl bromide is used as an example of the S_N1/S_N2 reactivity domain. Plotting initial rates against several initial NBB concentrations resulted in a good linear fit (Figure 2ii, $r^2 = 0.997$) and confirmed pseudo-first-order kinetics of the reaction of NBB with NBT. Table 2b gives the calculated rate constants and reaction orders for NBB and other S_N1/S_N2 type reactants.

Three electrophiles that included TDI, FDH, and IAA were evaluated as acylating agents, and the linear plot for TDI is given in Figure 2iii. The rate constants are shown in Table 2c. Pseudo-first-order kinetics was not observed with IAA, MSC, TDI, KTN, MITZ, and EtOX. However, the data for IAA, TDI, and MSC were able fit a second-order plot where the initial rates were plotted against $[E^+]^2$. KTN, MITZ, and EtOX exhibited complex behavior that fitted poorly into second-order plots.

Full Kinetics. The extent of the E^+−NBT reaction in terms of the depletion of NBT was measured at different time intervals (seconds or minutes) depending on the reaction rate. Data from complete reactions for all of the chemicals in the three domains were evaluated to obtain the overall rate constants. Pseudo-first-

Table 1. Test Chemicals That Were Reacted with NBT[a]

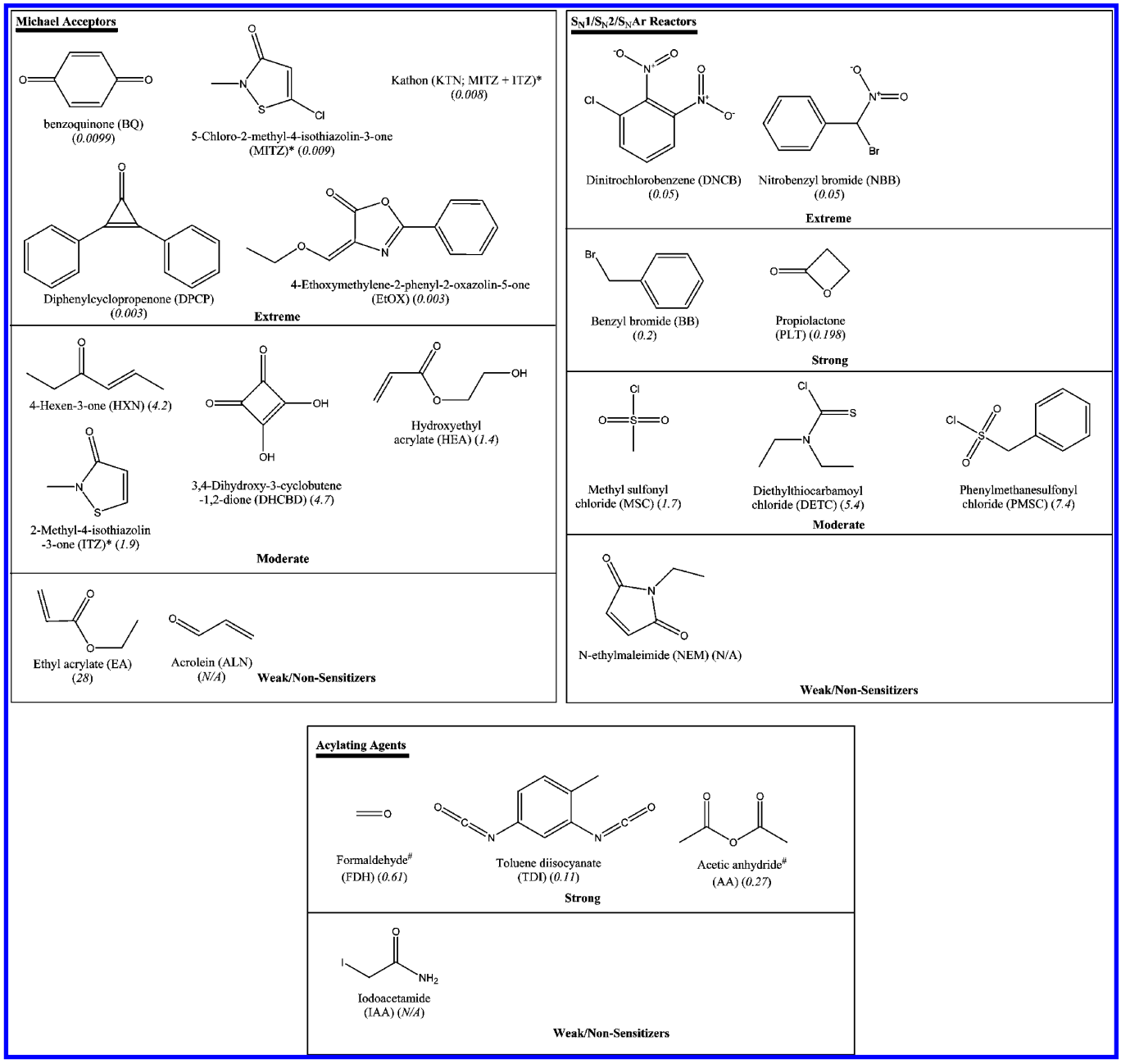

[a] Reported EC3 values for the chemicals (in parentheses) were adopted from previous studies (*12, 19*−*21*). * LC-MS analysis has indicated adduct formation inconsistent with Michael addition (*14*). # Even though formaldehyde and acetic anhydride are Schiff base formers, they were reactive to NBT.

order conditions were used with the E^+ in excess over the NBT. For the overall reaction, the NBT depletion data for several initial concentrations of the electrophiles (E^+) were fitted into the following integrated rate law for eq 2

$$\ln([\mathrm{NBT}] - [\mathrm{NBT}]_\infty) = -k't + \ln[\mathrm{NBT}]_0 \qquad (3)$$

where $k' = k_a[E^+]_0$. The value of the pseudo-first-order rate (k_a) was then calculated for given $[E^+]_0$ values. Pseudo-first-order plots for BQ, NBB, and TDI are given in Figure 3i−iii as examples of the reactivity of chemicals in the Michael acceptor, S_N1/S_N2, and acylating agents domains, respectively. In cases where linear curve fitting was not possible, quadratic regression was used, and the x coefficient was adopted as the slope (k') as has been reported by Roberts and Natsch (*14*). Table 3a−c lists all of the k_a values obtained for the three domains for varying $[E^+]_0$ values.

Elimination of possible depletion of NBT from competing side reactions such as oxidation and disulfide formation was achieved by varying initial $[E^+]_0$ and then plotting the slopes ($-k_s[E^+]_0$), obtained from plots of data fitted into eq 3 against $[E^+]_0$. Pseudo-first-order kinetics for overall NBT loss were calculated on the basis of the E^+-NBT reaction while assuming the loss of NBT due to side reactions such as oxidation/disulfide formation to be negligible ($k_i \ll k_s$) within the overall reaction time.

$$\frac{-\mathrm{d}[\mathrm{NBT}]}{\mathrm{d}t} = k_a[E^+]_0[\mathrm{NBT}]_0 + k_i[\mathrm{NBT}] \qquad (4)$$

Thus the equation was reduced to

$$\frac{\mathrm{d}[\mathrm{NBT}]}{\mathrm{d}t} = -k_a[E^+]_0[\mathrm{NBT}]_0 \qquad (2)$$

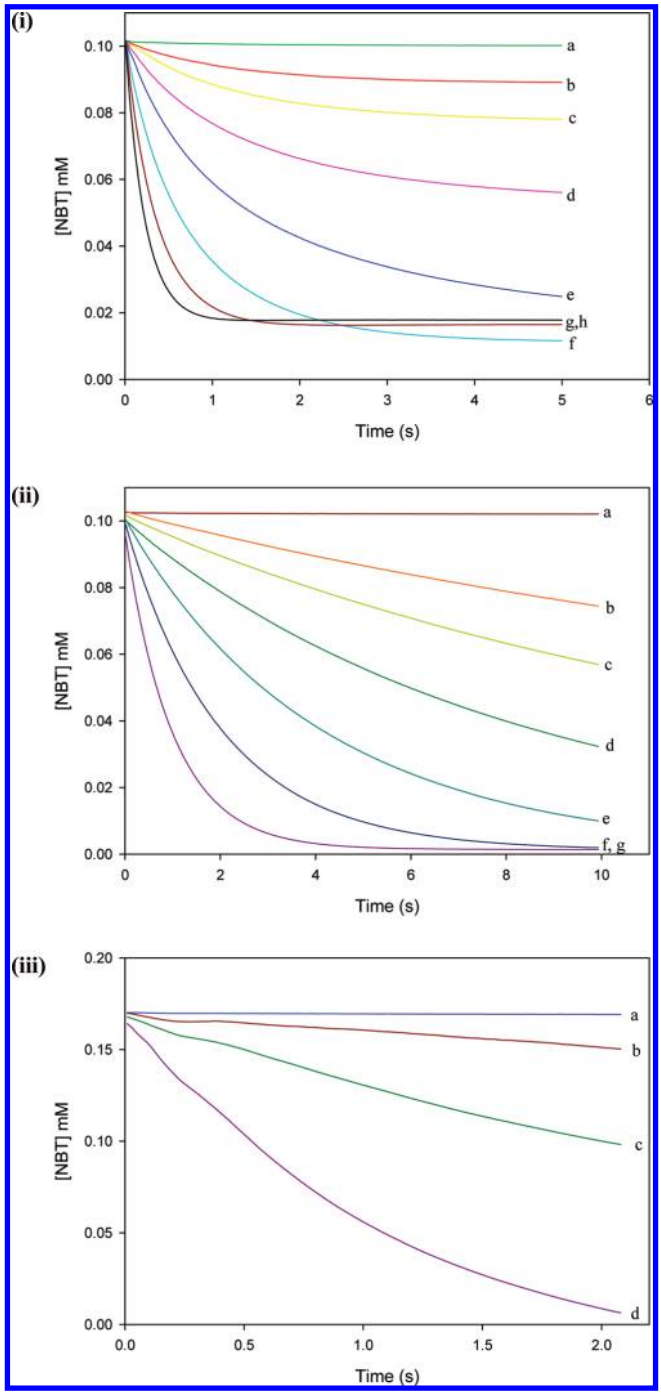

Figure 1. (i) Reaction of BQ with NBT in 50% ACN in a pH 7.4 phosphate buffer at 25 °C. Absorbance readings were performed at 412 nm. Using $[NBT]_0 = 0.1$ mM. BQ concentrations were varied from (a) 0.0, (b) 0.0125, (c) 0.025, (d) 0.05, (e) 0.1, (f) 0.2, (g) 0.4, and (h) 0.8 mM. (ii) NBB was reacted with 0.1 mM NBT in a phosphate-buffered 50% ACN. Initial NBB concentrations were (a) 0.0, (b) 0.1, (c) 0.25, (d) 0.5, (e) 1, (f) 2, and (g) 4 mM. (iii) NBT at a concentration of 0.1 mM was reacted with (a) 0, (b) 0.01, (c) 0.02, and (d) 0.05 mM TDI in acetone.

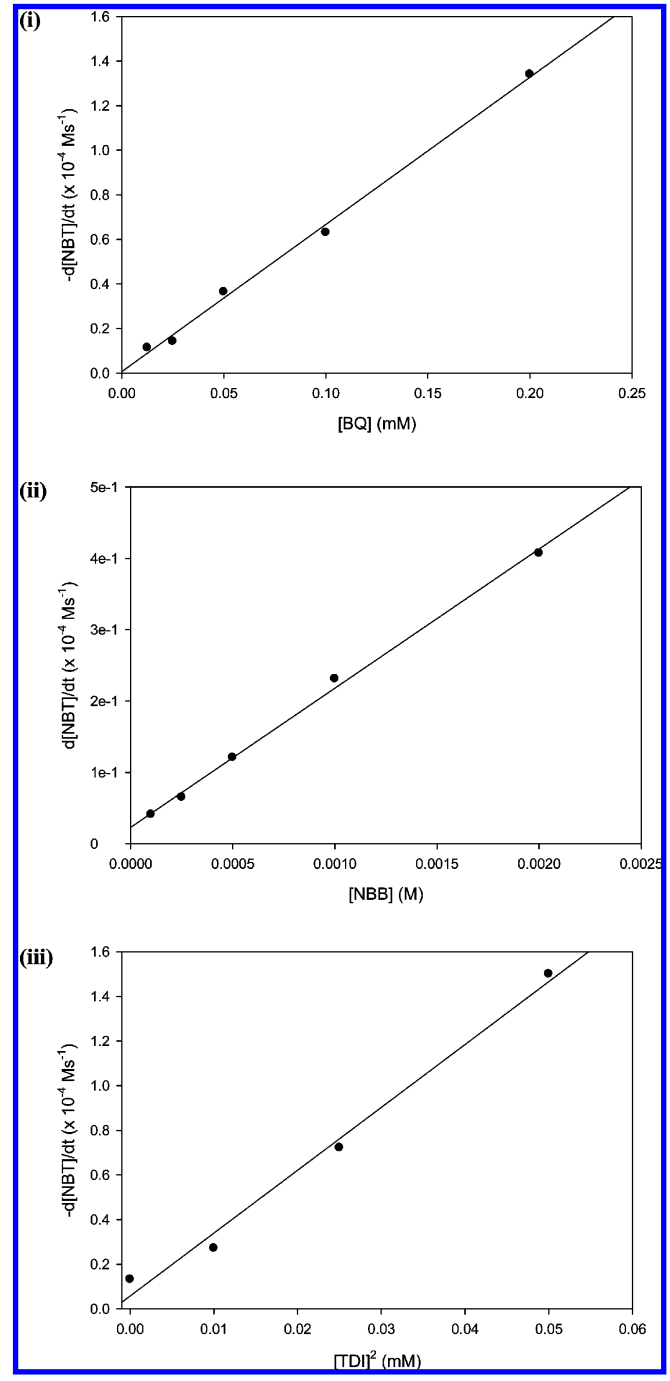

Figure 2. Initial rate vs $[E^+]$ plots for (i) BQ, (ii) NBB, and (iii) TDI. The rate constants are calculated from the slope of the $[E^+]$ vs initial rate for NBT depletion.

In cases where the NBT−E^+ reactions adhered to pseudo-first-order conditions, the pseudo-first-order rate constant ($k_s = -k_a[E^+]_0$) was calculated as the slope of the resultant linear curve ($[E^+]_0$ vs $-k_a[E^+]_0$), and the pseudo-first-order rate constant k_i for the side reaction was the intercept. Linear plots for BQ, NBB, and TDI are given in Figure 4i−iii. The values of k_s and k_i obtained using this method are listed in Table 3i−iii for comparison with k_a values. The values of the rate constants k_a and k_s were not significantly different between each chemical in all test mechanistic domains, even though the graphing method also resulted in the determination of k_i values.

Deviations from ideal pseudo-first-order conditions were observed with KTN, EtOX, MITZ, TDI, IAA, and MSC. TDI−NBT experiments were performed in acetone. Attempts to perform the reactions in either pure ACN or 1:1 ACN/PB resulted in immediate TDI precipitation. The closed reaction chamber of the stopped flow prevented evaporative loss of both the TDI and the acetone. The relatively large k_i (0.11 s^{-1}) for TDI (Table 3c) is indicative of a side reaction occurring concurrently with the NBT−TDI reaction.

Discussion

The development of alternative approaches to replace in vivo assays in skin sensitization testing is an important research area

Table 2. Rate Constants and Reaction Order Derived from the Initial Rate Methods for the (a) Michael Acceptor, (b) S_N1/S_N2, and (c) Acylating Agents Domains[a]

chemical	k (s^{-1})	r^2	order
	(a)		
BQ	0.696	0.996	1
KTN[b]	0.022	0.933	2
MITZ[b]	0.039	0.947	2
EA	1.7×10^{-6}	0.96	1
ITZ	0.0023	0.978	1
HEA	6.1×10^{-6}	0.95	1
ALN	2×10^{-5}	0.992	1
HNN	2×10^{-4}	0.989	1
DPCP	3×10^{-6}	0.99	1
DHCBD	2×10^{-5}	0.98	1
EtOX[b]	6×10^{-6}	0.956	2
	(b)		
BB	0.06	0.987	1
NBB	0.114	0.986	1
MSC[b]	0.0012	0.985	2
NEM	0.01	0.991	1
DETC	8.7×10^{-6}	0.997	1
PMSC	9×10^{-6}	0.993	1
PLN	1×10^{-5}	0.998	1
DNCB[c]	2.1×10^{-5}	0.993	1
	(c)		
TDI[b]	0.002	0.989	2
FDH	0.003	0.982	1
IAA[b]	3×10^{-7}	0.997	2
AA	0.0025	0.979	1

[a] The r^2 values are for the [E^+] vs initial rate of NBT depletion (d[NBT]/dt) under pseudo-first-order conditions. [b] KTN, MITZ, EtOX, TDI, MSC, and IAA were able to fit second-order plots. [c] DNCB has been known to react via an S_NAr reaction.

to protect the public from hazardous chemicals. A number of promising in vitro, in chemico, and in silico assays have been reported, and progress noted so far is due to the improved understanding of the skin sensitization processes at the molecular level (*15*). This study avails a simple spectrophotometric method capable of measuring rapid kinetics of common skin sensitizers with a select thiol-based nucleophile. Using stopped-flow and conventional UV−vis absorbance spectrophotometry, kinetics of 23 electrophilic chemicals reactivity to NBT were determined. Reactions ranged from very fast (BQ; $t_{1/2} = 0.4$ ms) to slow (EA; $t_{1/2} = 46.2$ s). The depletion of NBT, which has a high absorptivity coefficient at 412 nm, was studied under pseudo-first-order conditions. The use of ACN and acetone (in the case of TDI and DPCP) combined with a phosphate buffer eliminated the "drowning out effects", which Roberts and Natsch (*14*) observed with the HTKP assay. Solubility incompatibilities between the peptide and the chemicals sometimes resulted in "drowning out effects" of the chemicals (*14*). Inconsistencies due to the "drowning out effect" often result in discordant data for the same reactions. The model used herein benefited from comparative solubilities of NBT and the tested chemicals in the buffered organic solvent. The derivation of data was, thus, from solution kinetics, without the need to factor in the loss of reactants due to "drowning out effects". The accessible thiol group on NBT also enabled electrophile−nucleophile interactions with minimal steric hindrance from NBT. The stopped-flow measurements utilized a closed cell as the reaction chamber, and so, the effect of evaporative loss was absent. Evaporative loss has been cited as a contributing factor to discordant results in several chemistry-based assays and the LLNA (*14, 16*). Unlike the peptide reactivity assay (*10*), which was not sensitive for electrophilic chemicals at the high reactivity end, the stopped-flow method was able to capture a wide range of reaction rate constants.

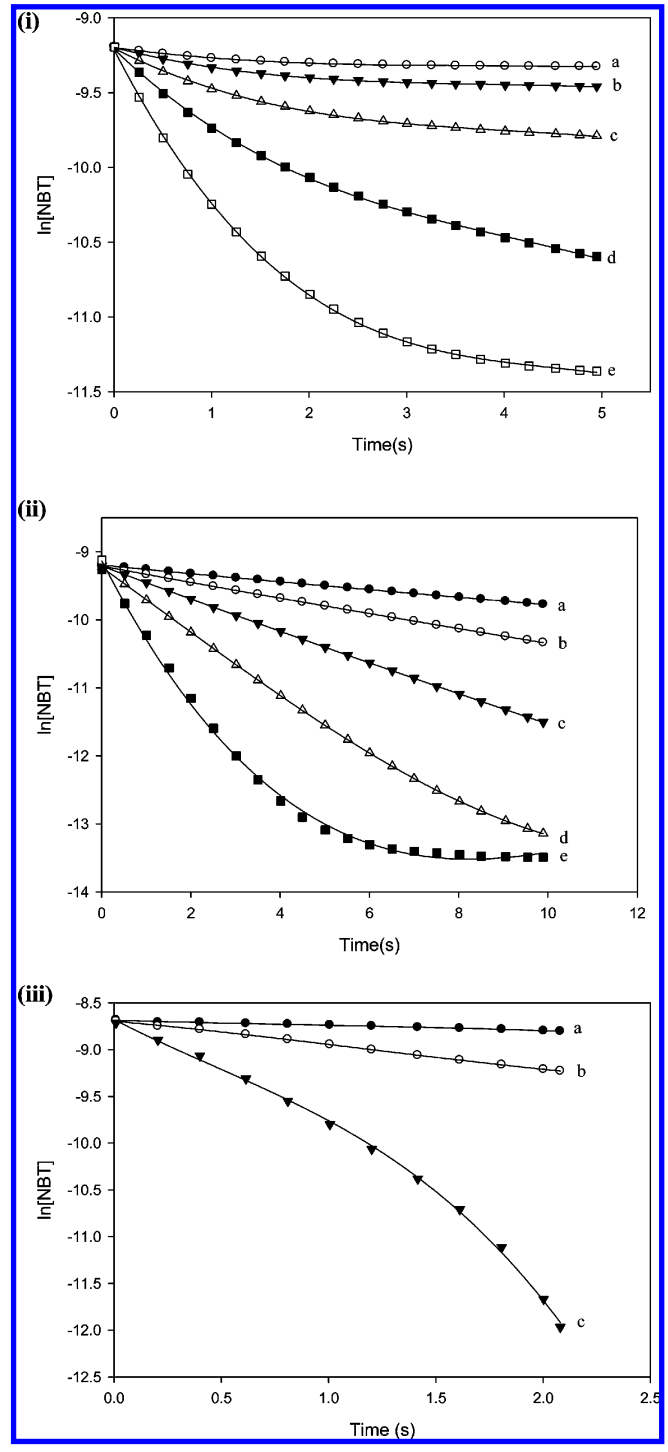

Figure 3. Pseudo-first-order plots for (i) BQ, (ii) NBB, and (iii) TDI representing the Michael acceptor, S_N1/S_N2, and acylating domains, respectively. Data obtained from full kinetics were used to plot the depletion of NBT with time.

The chemicals investigated in this study were classified into three mechanistic domains, and rate constants were compared within the same domain. The use of NBT as the nucleophile and the same buffered organic solvent (except for TDI and DPCP) ensured that nucleophilic influence and solvent effects were the same for all of the chemicals evaluated. Most of the data adhered to pseudo-first-order kinetics, irrespective of whether initial rates or the integrated rate equation was used to determine the rate constants. Deviations from ideal pseudo-first-order kinetics were evident with TDI, KTN, MITZ, EtOX, MSC, and IAA. The behavior exhibited by TDI can be attributed to the instability of TDI whenever there are trace amounts of water.

Table 3. Rate Constants and for the (a) Michael Acceptor, (b) S_N1/S_N2, and (c) Acylating Agents Domains[a]

chemical	k_a (s^{-1})	k_s (s^{-1})	$t_{1/2}$ (s)	k_i (s^{-1})
		(a)		
BQ	1660 ± 86	1576.5	0.00044	0.0106
KTN	58.6 ± 5.3	51.46	0.013	0.0005
MITZ	193 ± 6	196	0.0035	6×10^{-5}
ITZ	7.2 ± 1.3	6.7	0.096	2×10^{-5}
EA	0.018 ± 0.002	0.015	46.2	1×10^{-5}
HEA	0.053 ± 0.01	0.047	14.7	8×10^{-5}
ALN	0.16 ± 0.02	0.1	4.95	5×10^{-5}
HNN	0.418 ± 0.13	0.37	1.66	0.0089
DPCP	1105 ± 96	1083	0.00063	2×10^{-5}
DHCBD	0.189 ± 0.02	0.175	3.67	3×10^{-6}
EtOX	1290 ± 117	1343	0.00054	8×10^{-4}
		(b)		
BB	248 ± 24.5	246.8	0.0028	0.0006
NBB	1280 ± 123	1170	0.00059	0.0074
MSC	21.4 ± 6.0	15.0	0.046	0.0041
NEM	37.1 ± 12.6	34.9	0.020	6×10^{-6}
DETC	6.21 ± 0.74	7.64	0.091	0.0002
PMSC	1.92 ± 0.34	2.2	0.36	4×10^{-5}
PLN	71.4 ± 7.3	84.6	0.0097	3×10^{-5}
DNCB	0.87 ± 0.20	0.93	0.75	2×10^{-6}
		(c)		
TDI	20.1 ± 3.4	25.5	0.027	0.11
FDH	0.93 ± 0.78	8.3	0.075	0.013
IAA	3.53 ± 0.71	6.3	0.11	3×10^{-5}
AA	11.76 ± 1.64	12.07	0.059	5.3×10^{-3}

[a] Rate constants k_a were derived from the overall kinetics for the E^+-NBT reactions using eq 3. Rate constants k_s and k_i were determined as the slope and intercept of the linear plot of $[E^+]$ vs k' according to the integrated rate eq 3.

Rapid TDI hydrolysis results in amine formation. While the use of acetone may have slowed down the hydrolysis of TDI, the presence of side reactions was still evident as shown by the k_i value (Table 3c). The reaction dynamics for KTN were complex and exhibited a shift in the kinetics after the initial part of the reaction. Recent NMR studies (*17*) characterizing the peptide reactivity of the isothiazolinones that comprise KTN demonstrated the complex nature of KTN reactivity after the initial reactions. KTN exists as a mixture of two NBT reactive compounds (1.1% 5-chloro-2-methyl-4-isothiazolin-3-one and 0.4% 2-methyl-4-isothiazolin-3-one) in water. Thus, KTN composition may have resulted in two competing reactions with NBT resulting in deviations from ideal kinetics. The data from the NBT−KTN experiments were still able to fit into a second-order plot, albeit poorly, from which the rate constant (k_s) in Table 3a was derived. Further analysis of the reactivity of KTN can be done by analyzing the reactivity of the constituents of the KTN separately. Careful consideration of the percentages of the reactive constituents will result in data that can be used to derive more accurate rate constants for KTN. MSC and IAA were able to fit into second-order plots from which the rate constants were determined.

The different pH conditions between the surface of the stratum corneum (pH 5.5) and the epidermis (pH 7.4) have resulted in many speculations as to the role that pH plays in carrier protein haptenation (*7*). The degree of ionization of amino acids is pH-dependent and thereby affects nucleophilic reactivity to electrophilic chemicals. Kinetics measurements that were carried out at pH 5.5 highlighted the importance of the ionization state of NBT and the role of H^+ ions in the NBT−E^+ reaction. For BQ and MITZ, kinetics performed at pH 5.5 showed that the rate of the reaction increased ≈10-fold over the kinetics performed at pH 7.4 (data not shown). Lower pH is more relevant if protein haptenation is confined to and controlled by the microenvironment around the functional group of importance

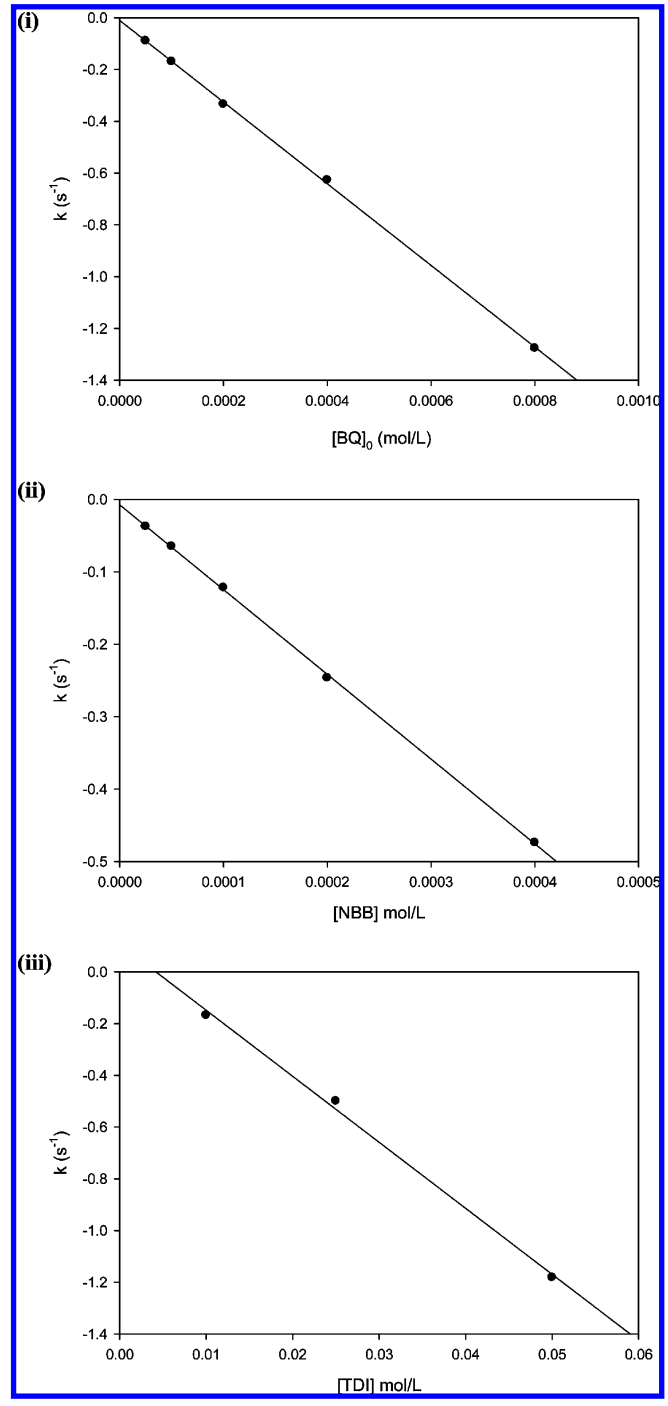

Figure 4. Linear plots for k' ($-k_s[E^+]_0$) vs (i) [BQ], (ii) [NBB], and (iii) [TDI]. The k_s values obtained from the slopes of the linear plots were agreeable to the k_a values obtained using eq 3. The intercepts of the linear plots are the rate constants (k_i) for any competing reactions.

on a protein. It has been argued that the microenvironment pH around a protein tends to be different from the overall physiological pH (*7*).

In comparison, the work done by Schultz et al. (*18*) argued that reactivity to GSH provided a good model for toxicity producing reactions of offending electrophiles with proteins and if classified in appropriate domains (e,g S_N1, S_N2, Michael acceptors, etc.) reactivity to nucleophiles such as GSH, and by extension, NBT tends to give a good indication of the reactivity of a chemical to cutaneous proteins. The relevance of the calculated rate constants to the chemicals' potency as skin sensitizers was outlined by plotting pEC3 values against log

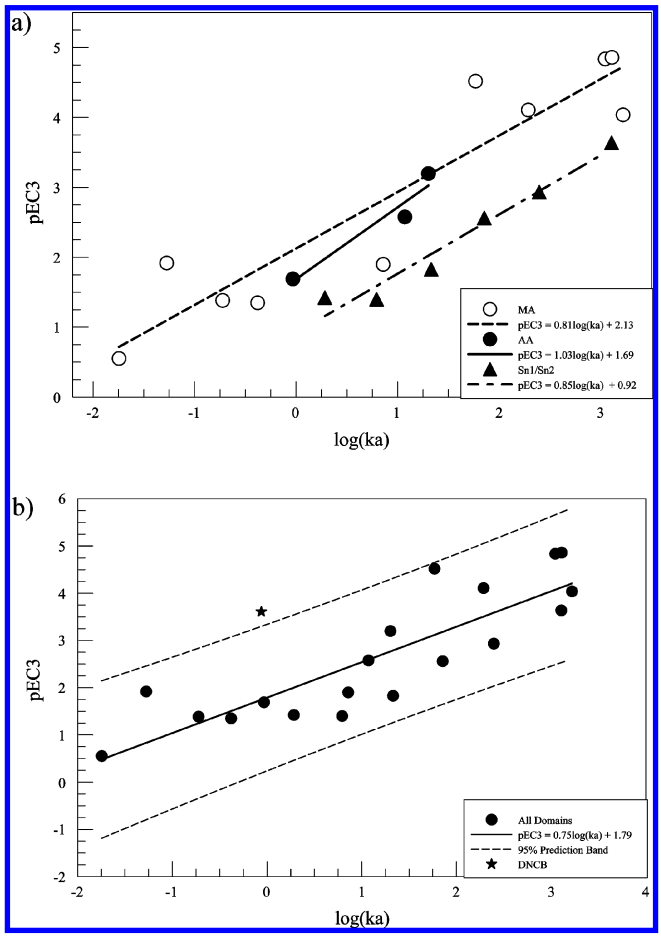

Figure 5. (a) Log k_a vs pEC3 for Michael acceptors, acetylating agents, and S_N1/S_N2 reactivity domains. Significant positive correlations between LLNA pEC3 values and NBT reactivity were observed within the domains. (b) Correlation between NBT reactivity and potency in the LLNA was still observed across all reactivity domains ($r^2 = 0.74$). DNCB NBT reactivity was observed but was outside the predictive bands at 95% CI.

k_a. The values for pEC3 were determined by dividing the molecular mass for the test chemical by the EC3 value and finding the log (*14*). Plots of pEC3 versus log k_a for the Michael acceptor, S_N1/S_N2, and acylating agent domains are shown in Figure 5a,b using rate constants in Table 3a−c and previously reported EC3 values (*12, 19−21*). Within the three domains and when all of the domains were combined (Figure 5b), there is a positive correlation between potency in the LLNA and reactivity to NBT as was indicated by the following linear equations (with statistical parameters)

$$\text{pEC3} = 0.81(\pm 0.11) \log k_a + 2.13(\pm 0.23) \qquad (6)$$

where $R^2 = 0.87$, $n = 10$, $R^2(\text{adj}) = 0.85$, $s = 0.65$, and $F = 52.3$.

$$\text{pEC3} = 0.85(\pm 0.09) \log k_a + 0.92(\pm 0.16) \qquad (7)$$

where $R^2 = 0.96$, $n = 6$, $R^2(\text{adj}) = 0.95$, $s = 0.20$, and $F = 93.7$.

$$\text{pEC3} = 1.03(\pm 0.27) \log k_a + 1.69(\pm 0.27) \qquad (8)$$

where $R^2 = 0.93$, $n = 3$, $R^2(\text{adj}) = 0.87$, $s = 0.27$, and $F = 14.23$.

$$\text{pEC3} = 0.75(\pm 0.11) \log k_a + 1.79(\pm 0.21) \qquad (9)$$

where $R^2 = 0.74$, $n = 19$, $R^2(\text{adj}) = 0.72$, $s = 0.71$, $F = 47.2$.

The linear equations were from the plots of the Michael acceptor (eq 6), S_N1/S_N2 (eq 7), acylating agent (eq 8), and all domains (eq 9), respectively. The correlation between pEC3 and log k within the Michael acceptor domain may weaken as more test chemicals are included due to the fact that the domain is structurally diverse; hence, reactivity to thiols differs within subsets of the domain. This was demonstrated in the GSH chemoassay where compounds with similar RC_{50} values were shown to have a 10-fold difference in rate constants (*22*). The allocation of Michael acceptors into subcategories of the domain (*23*) demonstrates this structural diversity. Data from the NBT−DNCB reaction shows that it was an outlier (Figure 5b). Given its potency classification as an extreme sensitizer with an EC3 value of 0.05%, DNCB would have been expected to react rapidly with NBT. DNCB, however, shows a slow reaction rate relative to the NBB (EC3 = 0.05%). While both react with NBT via a substitution mechanism, thiol attack on DNCB is on the benzene ring (S_NAr) as opposed to NBB, where nucleophilic attack is on the methyl C atom attached to the bromine. The attack on the ring proceeds more slowly than on the alkyl C atom. One explanation would be steric hindrance due to the nitro group adjacent to the chlorine. The reactivity rate of nitrochlorobenzene (NCB) to NBT was measured to evaluate this possibility. The overall rate ($k_a = 0.39\ s^{-1}$) of the NCB−NBT reaction was lower than that of DNCB ($k_a = 0.87\ s^{-1}$), suggesting that steric hindrance was not a determining factor in the DNCB−NBT reaction. The fact that the kinetics of the DNCB−NBT reaction was faster than the NCB−NBT reaction can be attributed to the inductive effect of the two electron-withdrawing nitro groups on DNCB as compared to NCB with one nitro group. The inclusion of DNCB, an S_NAr reactor, in a largely S_N1/S_N2 domain further highlights the resultant weak correlation between log k_a and pEC3 when data sets are not subcategorized.

Comparison of this model with existing kinetics profiling approaches shows that the new UV/vis-based method is superior with respect to the detectable range of electrophilic reactivity and to confounding factors such as potential loss of nucleophile due to oxidation. When the kinetics data were fitted into eq 3, comparison of the calculated rate constants k_s and k_i for the NBT−E^+ and side reactions, respectively, showed that $k_s \gg k_i$ in most cases (Table 3a−c); hence, contribution of the side reactions was negligible. TDI proved to be an exception with a significantly high k_i value of $0.11\ s^{-1}$. TDI rapidly hydrolyzes in trace amounts of aqueous media to give the urea product (*24*).

False negative results were obtained with known skin sensitizers that are cyclic anhydrides and diones like trimellitic anhydride and butanedione, respectively. The reactivity of formaldehyde and acetic anhydride to NBT was also interesting, given that these chemicals are Schiff base formers with preferential reactivity to amine-based nucleophiles, although their NBT reactivity potency rankings still were within the 95% prediction bands. The inclusion of an amine-based (harder) nucleophile to complement the softer thiol-based NBT would certainly reduce the false negatives obtained from non-NBT reactive chemical sensitizers like trimellitic anhydride. The present assay system correctly ranked HEA ($k_a = 0.053\ s^{-1}$; EC3 = 1.4) as more potent than EA ($k_a = 0.018\ s^{-1}$; EC3 = 28) within one degree of potency difference from reported EC3 values (3-fold NBT reactivity rate constant vs the 20-fold difference in the EC3 values between EA and HEA). Peptide reactivity studies using HEA and EA reported similar reactivities for these haptens (*25*). It was suggested that the LLNA results

for EA may be skewed due to potential free radical-induced polymerization and evaporative loss from the skin.

Our current method dwelled on the depletion of NBT with the assumption that the E^+−NBT reactions were characterized by adduct formation. While this may not have been the case with all test chemicals, peptide binding studies (*12, 22*), which have included characterization of the chemistry involved, have demonstrated oxidation of the peptide thiol as the substitute reaction whenever there was absence of adduct formation. The buffered organic media precluded oxidation of NBT to species other than the disulfide—of which the rate would have been slower than the E^+−NBT reaction. The fact that $k_s \gg k_i$ highlights the negligible contribution of disulfide formation to the overall depletion of NBT within the time frame of the reactions. Adduct formation with a protein is more important than oxidation of amino acid functional groups, as it results in a recognizable immunogen. The present assay, which captures adduct formation without interference from side reactions like oxidations, is of greater utility than the previously reported assays where complications arose from side reactions. Our study focused on the rapid depletion of NBT as a measure of the reactivity of test chemicals to nucleophiles, and just as argued by Mutschler et al. (*17*) in the reaction of three peptides with Kathon, the identification of adducts, while relevant, may not need to be the main focus in the development of an in chemico assay because it is complicated and sometimes misleading. Characterization of hapten−peptide adducts does not take into account the rapid reactivity (such as hydrolysis) of the identified adducts as was observed in Mutschler et al.'s study (*17*). Depletion of nucleophiles like NBT suffices as a simpler and relevant method for inclusion into a battery of preliminary screening assays for skin sensitizers. This study thus serves to strengthen other reported nucleophile depletion assays by capturing skin sensitizers with a wide range of reactivity. The study is particularly useful in measuring kinetics of rapidly reacting skin sensitizers and eliminates the need for estimated rate constants.

Acknowledgment. This work was supported by an Interagency Agreement with the NIEHS (#Y1-ES0001-06) and funding from NSF grant CHE0619224. The findings and conclusions in this report are those of the authors and do not necessarily represent the views of the National Institute for Occupational Safety and Health.

References

(1) Dean, J. H., Twerdok, L. E., Tice, R. R., Sailstad, D. M., Hattan, D. G., and Stokes, W. S. (2001) ICCVAM evaluation of the murine local lymph node assay. Conclusions and recommendations of an independent scientific peer review panel. *Regul. Toxicol. Pharmacol. 34* (3), 258–273.

(2) Buehler, E. V. (1965) Delayed contact hypersensitivity in the guinea pig. *Arch. Dermatol. 91*, 171–177.

(3) Magnusson, B., and Kligman, A. M. (1969) The identification of contact allergens by animal assay. The guinea pig maximization test. *J. Invest. Dermatol. 52* (3), 268–276.

(4) Ryan, C. A., Gerberick, G. F., Gildea, L. A., Hulette, B. C., Betts, C. J., Cumberbatch, M., Dearman, R. J., and Kimber, I. (2005) Interactions of contact allergens with dendritic cells: Opportunities and challenges for the development of novel approaches to hazard assessment. *Toxicol. Sci. 88* (1), 4–11.

(5) Schultz, T. W., Carlson, R. E., Cronin, M. T., Hermens, J. L., Johnson, R., O'Brien, P. J., Roberts, D. W., Siraki, A., Wallace, K. B., and Veith, G. D. (2006) A conceptual framework for predicting the toxicity of reactive chemicals: modeling soft electrophilicity. *SAR QSAR Environ. Res. 17* (4), 413–428.

(6) Roberts, D. W., Aptula, A. O., Patlewicz, G., and Pease, C. (2008) Chemical reactivity indices and mechanism-based read-across for non-animal based assessment of skin sensitisation potential. *J. Appl. Toxicol. 28* (4), 443–454.

(7) Divkovic, M., Pease, C. K., Gerberick, G. F., and Basketter, D. A. (2005) Hapten-protein binding: from theory to practical application in the in vitro prediction of skin sensitization. *Contact Dermatitis 53* (4), 189–200.

(8) Aleksic, M., Pease, C. K., Basketter, D. A., Panico, M., Morris, H. R., and Dell, A. (2008) Mass spectrometric identification of covalent adducts of the skin allergen 2,4-dinitro-1-chlorobenzene and model skin proteins. *Toxicol. in Vitro 22* (5), 1169–1176.

(9) Schultz, T. W., Yarbrough, J. W., and Johnson, E. L. (2005) Structure-activity relationships for reactivity of carbonyl-containing compounds with glutathione. *SAR QSAR Environ. Res. 16* (4), 313–322.

(10) Gerberick, G. F., Vassallo, J. D., Bailey, R. E., Chaney, J. G., Morrall, S. W., and Lepoittevin, J. P. (2004) Development of a peptide reactivity assay for screening contact allergens. *Toxicol. Sci. 81* (2), 332–343.

(11) Gerberick, G. F., Vassallo, J. D., Foertsch, L. M., Price, B. B., Chaney, J. G., and Lepoittevin, J. P. (2007) Quantification of chemical peptide reactivity for screening contact allergens: A classification tree model approach. *Toxicol. Sci. 97* (2), 417–427.

(12) Natsch, A., and Gfeller, H. (2008) LC-MS-based characterization of the peptide reactivity of chemicals to improve the in vitro prediction of the skin sensitization potential. *Toxicol. Sci. 106* (2), 464–478.

(13) Natsch, A., Gfeller, H., Rothaupt, M., and Ellis, G. (2007) Utility and limitations of a peptide reactivity assay to predict fragrance allergens in vitro. *Toxicol. in Vitro 21* (7), 1220–1226.

(14) Roberts, D. W., and Natsch, A. (2009) High throughput kinetic profiling approach for covalent binding to peptides: Application to skin sensitization potency of michael acceptor electrophiles. *Chem. Res. Toxicol. 22* (3), 592–603.

(15) Jowsey, I. R., Basketter, D. A., Westmoreland, C., and Kimber, I. (2006) A future approach to measuring relative skin sensitising potency: A proposal. *J. Appl. Toxicol. 26* (4), 341–350.

(16) Siegel, P. D., Fedorowicz, A., Butterworth, L., Law, B., Anderson, S. E., Snyder, J., and Beezhold, D. (2009) Physical-chemical and solvent considerations in evaluating the influence of carbon chain length on the skin sensitization activity of 1-bromoalkanes. *Toxicol. Sci. 107* (1), 78–84.

(17) Mutschler, J., Gimenez-Arnau, E., Foertsch, L., Gerberick, G. F., and Lepoittevin, J. P. (2009) Mechanistic assessment of peptide reactivity assay to predict skin allergens with Kathon CG isothiazolinones. *Toxicol. in Vitro 23* (3), 439–446.

(18) Schultz, T. W., Ralston, K. E., Roberts, D. W., Veith, G. D., and Aptula, A. O. (2007) Structure-activity relationships for abiotic thiol reactivity and aquatic toxicity of halo-substituted carbonyl compounds. *SAR QSAR Environ. Res. 18* (1−2), 21–29.

(19) Gerberick, G. F., Ryan, C. A., Kern, P. S., Schlatter, H., Dearman, R. J., Kimber, I., Patlewicz, G. Y., and Basketter, D. A. (2005) Compilation of historical local lymph node data for evaluation of skin sensitization alternative methods. *Dermatitis 16* (4), 157–202.

(20) van Och, F. M., Slob, W., de Jong, W. H., Vandebriel, R. J., and van, L. H. (2000) A quantitative method for assessing the sensitizing potency of low molecular weight chemicals using a local lymph node assay: Employment of a regression method that includes determination of the uncertainty margins. *Toxicology 146* (1), 49–59.

(21) Chipinda, I., Hettick, J. M., Simoyi, R. H., and Siegel, P. D. (2008) Zinc diethyldithiocarbamate allergenicity: Potential haptenation mechanisms. *Contact Dermatitis 59* (2), 79–89.

(22) Bohme, A., Thaens, D., Paschke, A., and Schuurmann, G. (2009) Kinetic glutathione chemoassay to quantify thiol reactivity of organic electrophiles—Application to alpha, beta-unsaturated ketones, acrylates, and propiolates. *Chem. Res. Toxicol. 22* (4), 742–750.

(23) Schultz, T. W., Rogers, K., and Aptula, A. O. (2009) Read-across to rank skin sensitization potential: Subcategories for the Michael acceptor domain. *Contact Dermatitis 60* (1), 21–31.

(24) Chipinda, I., Stetson, S. J., Depree, G. J., Simoyi, R. H., and Siegel, P. D. (2006) Kinetics and mechanistic studies of the hydrolysis of diisocyanate-derived bis-thiocarbamates of cysteine methyl ester. *Chem. Res. Toxicol. 19* (3), 341–350.

(25) Dearman, R. J., Betts, C. J., Farr, C., McLaughlin, J., Berdasco, N., Wiench, K., and Kimber, I. (2007) Comparative analysis of skin sensitization potency of acrylates (methyl acrylate, ethyl acrylate, butyl acrylate, and ethylhexyl acrylate) using the local lymph node assay. *Contact Dermatitis 57* (4), 242–247.

TX100003W